Numerical Algorithms (2021) 87:137–160
https://doi.org/10.1007/s11075-020-00961-2

ORIGINAL PAPER

A central-line coarse preconditioner for Stokes flows in artery-like domains

Yingzhi Liu[1] · **Xiao-Chuan Cai**[2]

Received: 29 October 2019 / Accepted: 3 June 2020 / Published online: 3 July 2020

Abstract
We consider numerical simulation of blood flows in the artery using multilevel domain decomposition methods. Because of the complex geometry, the construction and the solve of the coarse problem take a large percentage of the total compute time in the multilevel method. In this paper, we introduce a one-dimensional central-line model of the blood flow and use its stabilized finite element discretization to construct a coarse preconditioner. With suitable restriction and extension operators, we obtain a two-level additive Schwarz preconditioner for two- and three-dimensional problems. We present some numerical experiments with different arteries to show the efficiency and robustness of the new coarse preconditioner whose computational cost is considerably lower than other coarse preconditioners constructed using the two- or three-dimensional geometry of the artery.

Keywords Stokes problem · Blood flow in artery · Multilevel domain decomposition · Central-line coarse space · Finite element

Mathematics subject classification (2010) 76D07 · 65N30 · 65N55 · 65Y05

1 Introduction

Computational fluid dynamics (CFD) is increasingly used to study blood flows in human arteries. Such numerical simulations are important for the understanding of

✉ Xiao-Chuan Cai
xccai@um.edu.mo

Yingzhi Liu
yzhil90@gmail.com

[1] School of Mathematics and Statistics, Xi'an Jiaotong University, Xi'an, 710049, People's Republic of China

[2] Department of Mathematics, University of Macau, Macau, Macau

the flow behavior and also for the planning for surgery. However, the computation is often time consuming; thus, large scale computers and multilevel algorithms are necessary. In traditional multilevel domain decomposition methods, if the artery is assumed to be in R^d ($d = 2, 3$), then the fine and coarse meshes are both in R^d, even if the number of coarse grid points is much smaller than the number of fine grid points; the coarse problem may become expensive to solve for arteries with many branches and for parallel computers with many processor cores. In this paper, we take the advantage of the fact that the artery tree looks one-dimensional if we assume the length is much longer than the cross-section and design a coarse space associated with the one-dimensional central line of the artery. With proper restriction and interpolation, this one-dimensional coarse preconditioner can be integrated into a two- and three-dimensional preconditioner easily. We focus on the linear Stokes problems defined on an artery-like domain and develop a fully coupled multiscale overlapping additive Schwarz domain decomposition method whose subdomain preconditioners are in R^d, but the coarse preconditioner is in R^1.

There are many numerical methods for solving Stokes problems. For example, A. Klawonn et al. presented a block-diagonal preconditioner in [21] by fully decoupling the velocity field and the pressure field. Subsequently, the authors showed a partially coupled block-triangular preconditioner and a fully coupled additive Schwarz preconditioner in [22, 23] and then provided a comparison of these preconditioners in [24]. In [23], both the subdomain problems and coarse problem are derived from the original saddle-point problem in overlapping subdomains with a fine mesh and the original domain with a coarse mesh. The paper also showed that the fully coupled approach is faster than the partially coupled and the fully decoupled approaches. For the time-dependent Stokes problems with small time step size, L.F. Pavarino further pointed out that the block-diagonal and block-triangular preconditioners do not work as well as the fully coupled method [30]. Note that the coarse spaces of all the aforementioned preconditioners are constructed in coarse meshes in R^d, where d is the dimension of the original problem, which means that the coarse solve will become very expensive for arteries with many branches. In addition, as shown in [25, 26], such a coarse mesh needs to preserve the same geometry as the fine mesh on the boundary, which is not easy for most existing coarsening algorithms. The same high cost coarse preconditioning issue appears in other substructuring domain decomposition methods such as dual-primal FETI method [20, 28] and BDDC methods [29, 31]. We note that optimized Schwarz methods have been studied for circular or cylindrical domains that can be viewed as an artery without branching [14–16]. We also mention that there are other methods for solving saddle-point problems including Uzawa's methods [5, 9], multigrid methods [8, 40, 41], and Hermitian and skew-Hermitian splitting methods [1–3]. Interested readers should refer to [4] for a comprehensive introduction.

Not as a preconditioner, but as a cheap approximation of the full three-dimensional model, the one-dimensional central-line model has been quite popular for studying blood flows because of its lower computational cost [13, 32–34, 36–38]. The one-dimensional model in compliant arteries whose wall deforms under the action of the blood flow is derived by writing the basic conservation laws into integral forms and then applying certain homogenization techniques across the axial section of the

artery [13, 32]. This applies to non-bifurcating and also arterial networks with special attention for the cross-sections near the bifurcations [11, 36]. The one-dimensional models have been successfully used to investigate the effects on the blood flow of the geometrical and mechanical arterial modification, due to the presence of stenoses, or the placement of stents or prostheses [6, 12, 35]. N. Smith et al. applied the one-dimensional model to the coronary arteries in [37] and later developed the model for the coronary microvascular networks considering the change of the viscosity of blood in [27]. A. Quarteroni et al. introduced the multiscale model of the entire circulatory system by coupling the three-, one-, and zero-dimensional models together [10, 13, 33].

Compared with the one-dimensional models, two- and three-dimensional Stokes or Navier-Stokes models provide higher physical fidelity but are computationally much more expensive. In this paper, we consider the Stokes flows in arteries, and we design a fully coupled two-level additive Schwarz preconditioner in which the coarse preconditioner is constructed by a discretization of a one-dimensional model on the central line. Very different from the classical coarse preconditioners defined using the original model on a coarse mesh, the central-line coarse preconditioner maintains nearly the same efficiency and robustness as high dimensional coarse preconditioners but has a very low computational cost.

The paper layout is as follows. In Section 2, we show the model and its stabilized finite element discretization. In Section 3, we introduce the one-dimensional model for the Stokes problem in a single vessel domain, then present a multiscale two-level additive Schwarz preconditioner subdomain preconditioners defined in R^d and coarse preconditioner in R^1. In Section 4, we provide some analysis of the condition number of the preconditioned matrix for elliptic problems defined on artery-like domains. Finally, we show some numerical experiments for Stokes and elliptic problems defined on several different arteries.

2 Model problems and their stabilized finite element discretizations

We first consider the steady-state Stokes problem [17] in $R^d (d = 2, 3)$,

$$\begin{cases} -\nu\Delta u + \nabla p = f \ \text{ in } \ \Omega, \\ \nabla \cdot u = 0 \ \text{ in } \ \Omega, \\ u = g \ \text{ on } \ \Gamma, \end{cases} \tag{1}$$

where $u = (u_1, u_2, \cdots, u_d)^T$ is the velocity, $f = (f_1, f_2, \cdots, f_d)^T$ is the source force, and p is the pressure. We assume $\Omega \subset R^d$ is an artery-like domain (see Fig. 1) with a polygonal boundary Γ. For the pressure variable, we impose the condition $\int_\Omega p dx = 0$ so that the solution is unique.

We use the stabilized finite element method to discretize (1) on a given conforming triangular ($d = 2$) or tetrahedral ($d = 3$) mesh $\mathcal{T}_h = \{K\}$. For each element K, we denote by h_K as its diameter. Let V_h and P_h be a pair of finite element spaces for the velocity and pressure given by

$$V_h = \left\{ v \in (C^0(\Omega) \cap H^1(\Omega))^d : v|_K \in P_1(K)^d, K \in \mathcal{T}_h \right\}$$

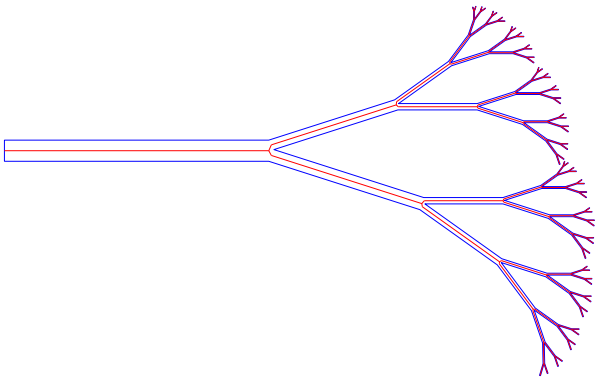

Fig. 1 An artery-like computational domain and the central line is marked in red

and

$$P_h = \left\{ q \in C^0(\Omega) \cap L^2(\Omega) : q|_K \in P_1(K), K \in \mathcal{T}_h \right\},$$

where $C^0(\Omega)$ is the continuous function space, $L^2(\Omega)$ and $H^1(\Omega)$ are standard Sobolev spaces in the finite element literature [17], and $P_1(K)$ is the linear function space in element K. Furthermore, we define some related spaces as follows

$$V_{h,g} = \{v \in V_h : v|_\Gamma = g\}, \quad V_{h,0} = \{v \in V_h : v|_\Gamma = 0\},$$

and

$$P_{h,0} = \left\{ p \in P_h : \int_\Omega p dx = 0 \right\}.$$

Following [7, 18, 19], the stabilized finite element method for the steady-state Stokes problem is given as: Find $(u_h, p_h) \in V_{h,g} \times P_{h,0}$, such that

$$B(u_h, p_h; v, q) = F(v, q) \quad \forall (v, q) \in V_{h,0} \times P_{h,0} \tag{2}$$

with

$$\begin{aligned} B(u, p; v, q) = \; & (\nu \nabla u, \nabla v) - (\nabla \cdot v, p) - (\nabla \cdot u, q) \\ & -\alpha \sum_{K \in \mathcal{T}_h} h_K^2 (-\nu \Delta u + \nabla p, \epsilon \nu \Delta v + \nabla q)_K \end{aligned}$$

and

$$F(v, q) = (f, v) - \alpha \sum_{K \in \mathcal{T}_h} h_K^2 (f, \epsilon \nu \Delta v + \nabla q)_K.$$

Here, $\alpha > 0$ is a stabilization parameter and $\epsilon = 0, 1, -1$ correspond to SUPG [19], DW [7], GLS [18] stabilized finite element methods, respectively. As shown in [7, 18, 19], (2) has a stable solution with optimal convergence for any choice of positive α. We set $\alpha = 1$ throughout this paper. Because $u_h|_K, v|_K \in P_1(K)^d$, the terms Δu_h and Δv in $B(u, p; v, q)$ and $F(v, q)$ vanish. Let us denote the matrix form of (2) as

$$Ax = b, \quad A = \begin{pmatrix} A_\nu & B_{div}^T \\ B_{div} & M_p \end{pmatrix}, \tag{3}$$

where A_v, B_{div}, and M_p are the matrix forms of the first, third, and fourth terms of $B(u, p; v, q)$, respectively. Note that the matrix A is symmetric but indefinite. In this paper, we solve the linear system (3) by a right preconditioned Krylov subspace method, i.e.,

$$AP^{-1}y = b, \text{ with } x = P^{-1}y, \tag{4}$$

where P^{-1} is a preconditioner to be defined in the following section.

3 A multiscale two-level Schwarz preconditioner

In this section, we introduce a multiscale overlapping additive Schwarz preconditioner. The additive preconditioner takes the form $P^{-1} = P_c^{-1} + P_s^{-1}$, where P_c^{-1} is a one-dimensional preconditioner defined on the central line of the artery and P_s^{-1} is the sum of all the subdomain preconditioners.

3.1 One-dimensional flow model in artery-like domains

In this subsection, we define the one-dimensional coarse preconditioner. Following [32], we introduce some notations and assumptions about the artery-like computational domain (see Fig. 2) and also the Stokes equations.

(A1) The artery is axial symmetry with respect to the central line and its radius $r_0 = r_0(s)$ is a function along the axial direction s.

(A2) The wall is fixed or is not displaced with respect to the time. Therefore, the radius r_0 is independent of time t.

(A3) The pressure p is constant on each axial section $C_s(s)$.

(A4) The velocity components orthogonal to the axial direction s are negligible compared to the component along s. Let r be radial coordinate of the axial section $C_s(s)$. Then, the axial component u_s can be expressed as

$$u_s(t, r, s) = \bar{u}_s(t, s)V_p\left(\frac{r}{r_0(s)}\right), \tag{5}$$

where $\bar{u}_s$ is the mean velocity of u_s on axial section and $V_p : \mathbb{R} \to \mathbb{R}$ is a velocity profile.

Denote the central line $x(s) = (x_1(s), \cdots, x_d(s))$ as a parametric equation with respect to the axial direction s. Let $A_s = A_s(s)$ be the area of the axial section $C_s(s)$. Then, we have $A_s = 2r_0(s)$ for 2D and $A_s = \pi r_0^2(s)$ for 3D from the above assumptions. The mean velocity $\bar{u}_s$ is then given by

$$\bar{u}_s = A_s^{-1}\int_{C_s} u_s d\sigma.$$

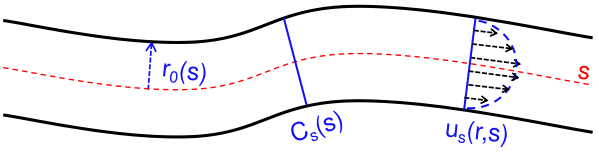

Fig. 2 Vascular diagram and some notations and assumptions used for in the one-dimensional model

The flux is defined as

$$Q = \int_{C_s} u_s d\sigma = A_s \bar{u}_s.$$

From the definitions of u_s, $\bar{u}_s$, and Q, it follows that

$$\int_0^1 V_p(y)dy = 1 \quad \text{for 2D;} \int_0^1 V_p(y)ydy = \frac{1}{2} \quad \text{for 3D.}$$

In this paper, we choose the profile law as a parabolic profile and then obtain from the above property

$$V_p(y) = \frac{3}{2}(1-y^2) \quad \text{for 2D;} \; V_p(y) = 2(1-y^2) \quad \text{for 3D;} \quad y \in [0,1]. \tag{6}$$

Let $\tau(s) = (\tau^1(s), \cdots, \tau^d(s))$ be the unit tangent vector of the central line and f be the source force. Then, we denote by $f_{cl} = \int_{C_s} f \cdot \tau d\sigma$.

For the time-dependent 3D Navier-Stokes equations in a single compliant vessel, the 1D model is delicately derived in [32] as

$$\begin{cases} \dfrac{\partial Q}{\partial t} + \alpha \dfrac{\partial}{\partial s}\left(\dfrac{Q^2}{A_s}\right) + \dfrac{A_s}{\rho}\dfrac{\partial p}{\partial s} + K_r \dfrac{Q}{A_s} = f_{cl}, \\ \dfrac{\partial A_s}{\partial t} + \dfrac{\partial Q}{\partial s} = 0, \end{cases} \tag{7}$$

where $A_s = A_s(t,s)$ is the time-dependent area, $\alpha = \int_{C_s} u_s^2 d\sigma / A_s \bar{u}_s^2 = \int_{C_s} V_p^2 d\sigma / A_s = 4/3$ is the Coriolis coefficient, and $K_r = -2\pi\nu V_p'(1) = 8\pi\nu$.

Remark 1 For the time-dependent 1D model, if we assume that the wall is elastic with constant Young modulus E and Poisson ratio v, then a typical relationship (cf. [13, 32]) between the pressure and the time-dependent vessel area $A_s(t)$ is

$$p(t) = p(0) + \frac{\sqrt{\pi} h_0 E}{(1-v^2)A_s(0)}\left(\sqrt{A_s(t)} - \sqrt{A_s(0)}\right), \tag{8}$$

where h_0, $p(0)$, and $A_s(0)$ are the vessel thickness, the pressure, and the section area at the initial time (the reference configuration), respectively.

Using a similar derivation and let u_{cl} and p_{cl} be the value of u_s and p on the central line, respectively, we can obtain the 1D model of the steady-state Stokes equations in a single vessel

$$\begin{cases} K_r u_{cl} + \dfrac{A_s}{\rho}\dfrac{\partial p_{cl}}{\partial s} = f_{cl}, \\ \dfrac{\partial (A_s u_{cl})}{\partial s} = 0, \end{cases} \tag{9}$$

where $K_r = -\dfrac{4}{3}\dfrac{\nu}{r_0}V_p'(1) = \dfrac{4\nu}{r_0}$ for 2D and $K_r = -\pi\nu V_p'(1) = 4\pi\nu$ for 3D.

Remark 2 Note that (9) is an ordinary differential equation for variable s. Therefore, its solution is unique if the values of u_{cl} and p_{cl} are given at the end of the central line.

For artery with bifurcation (see Fig. 3), we can consider it as a collection of single vessels. For each inlet or outlet of each vessel, we assume there is a flow rate and a pressure value that are either given (if it is a boundary) or as unknowns to be solved. When defining the central-line preconditioner, there are two approaches. In the first approach (see the left figure of Fig. 4), we treat each single vessel independently in the discretization using the flow rate and pressure values at both inlet and outlet as boundary conditions, and then by the conservation of the flux and the continuity of the pressure, we have [11]

$$Q_1 = Q_2 + Q_3, \quad p_{cl}^1 = p_{cl}^2 = p_{cl}^3.$$

Using the fact $Q_i = c_0 r_i^{d-1} u_{cl}^i$, we obtain

$$r_1^{d-1} u_{cl}^1 = r_2^{d-1} u_{cl}^2 + r_3^{d-1} u_{cl}^3, \quad p_{cl}^1 = p_{cl}^2 = p_{cl}^3.$$

To solve (u_{cl}^2, p_{cl}^2) and (u_{cl}^3, p_{cl}^3), for a given (u_{cl}^1, p_{cl}^1), we can use the relations

$$\begin{cases} r_2^{d-1} u_{cl}^2 = \xi_2 r_1^{d-1} u_{cl}^1, \\ p_{cl}^2 = p_{cl}^1, \end{cases} \quad \begin{cases} r_2^{d-1} u_{cl}^3 = \xi_3 r_1^{d-1} u_{cl}^1, \\ p_{cl}^3 = p_{cl}^1, \end{cases} \tag{10}$$

where ξ_2 and ξ_3 are nonnegative and satisfy $\xi_2 + \xi_3 = 1$. Similar relations hold for artery with more generations of branches. In the second approach (see the right figure of Fig. 4), the network of artery is not divided at the junctions. In such a way, the bifurcation points become the internal points of the arterial networks, and hence, the bifurcation conditions are not necessary. In the numerical experiments, we will compare these two approaches, and it turns out they perform more or less the same as a coarse preconditioner, and the first approach is often easier to implement. In the next subsection, we will discuss a finite element discretization of (9) and also show how to integrate it into a multilevel preconditioner in 2D and 3D.

Remark 3 In this paper, we only consider the case when the wall is rigid. The extension to the situation when the wall is deformable is, in theory, straightforward in the sense that we only need to change the definition of the cross-section area A_s in the algorithm, but the actual implementation could be complicated, and its effectiveness needs to be studied.

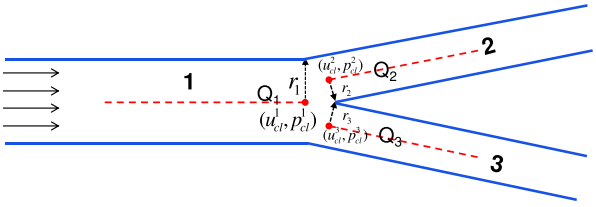

Fig. 3 Notations for an artery with a bifurcation

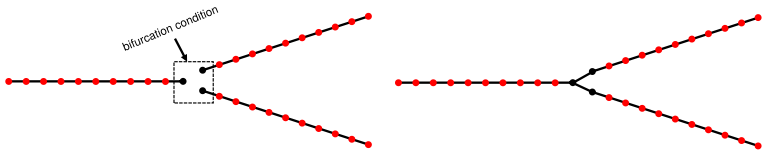

Fig. 4 An arterial network can be considered a collection of individual vessels with consistent inlet/outlet conditions for the flow rate and pressure (left) or as a single network (right) that satisfies a differential equation similar to (9)

3.2 A two-level additive Schwarz method with a central-line coarse preconditioner

In this subsection, we briefly recall the classical additive Schwarz method and then focus on the central-line coarse preconditioner. We first decompose the domain Ω into N nonoverlapping subdomains $\{\Omega_i\}_{i=1}^N$ or more precisely the finite element mesh $\mathcal{T}_h$ into $\mathcal{T}_{h,i}$. The overlapping subdomains $\{\Omega_i^\delta\}_{i=1}^N$ can be obtained by extending Ω_i with δ layers of elements from neighboring subdomains. Sometimes, we use $\mathcal{T}_{h,i}^\delta$ to denote the mesh on Ω_i^δ. Then, we define the subdomain velocity and pressure spaces as

$$V_h^i = \left\{ v \in V_h \cap (H^1(\Omega_i^\delta))^d : v = 0 \text{ on } \partial\Omega_i^\delta \right\}$$
$$P_h^i = \left\{ p \in P_h \cap L^2(\Omega_i^\delta) : p = 0 \text{ on } \partial\Omega_i^\delta \setminus \Gamma \right\}.$$

For simplicity, we extend all subdomain functions to the entire domain by zero such that V_h^i and P_h^i are subspaces of the V_h and P_h, respectively. On the physical boundaries, we impose Dirichlet conditions according to the original (1). On the artificial boundaries, we assume both $u = 0$ and $p = 0$.

Let $R_i : V_h \times P_h \to V_h^i \times P_h^i$ be a restriction operator which returns all degrees of freedom associated with the subspace $V_h^i \times P_h^i$. The extension operator R_i^T can be defined as the transpose of R_i. The subdomain matrix A_i can be obtained as $A_i = R_i A R_i^T$ or by discretizing the problem on the subdomain with approximate boundary conditions. Now, the one-level additive Schwarz preconditioner in the matrix form can be written as

$$P_{1s}^{-1} = \sum_{i=1}^{N} R_i^T A_i^{-1} R_i.$$

Next, we define the coarse matrix A_{cl} and the corresponding restriction operator R_{cl} and extension operator E_{cl} using the 1D flow model given in the previous subsection .

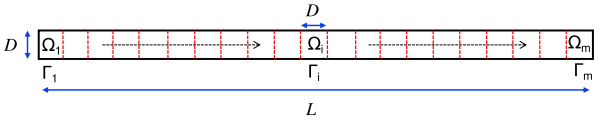

Fig. 5 A single vessel domain with a quasi-unform subdomain partition

Denote Ω_{cl} as the central line of Ω and $\mathcal{T}_H^{cl}$ as a one-dimensional finite element mesh of Ω_{cl} with mesh size H. As an extension of $\mathcal{T}_H^{cl}$, we introduce a coarse mesh $\mathcal{T}_H$ of Ω by extending each mesh point in $\mathcal{T}_H^{cl}$ across or approximately across the axial direction s and then joining these points by a delaunay triangulation.

Define the velocity and pressure spaces in $\mathcal{T}_H$ and $\mathcal{T}_H^{cl}$ as

$$V_H = \left\{ v \in (C^0(\Omega) \cap H^1(\Omega))^d : v|_K \in P_1(K)^d, K \in \mathcal{T}_H \right\},$$
$$P_H = \left\{ q \in C^0(\Omega) \cap L^2(\Omega) : q|_K \in P_1(K), K \in \mathcal{T}_H \right\},$$

and

$$V_H^{cl} = \left\{ v \in C^0(\Omega_{cl}) \cap H^1(\Omega_{cl}) : v|_K \in P_1(K), K \in \mathcal{T}_H^{cl} \right\},$$
$$P_H^{cl} = \left\{ q \in C^0(\Omega_{cl}) \cap L^2(\Omega_{cl}) : q|_K \in P_1(K), K \in \mathcal{T}_H^{cl} \right\}.$$

As in the fine mesh case, we can also define the restriction and extension operators R_f^c and $R_c^f = (R_f^c)^T$ for the coarse mesh $\mathcal{T}_H$. On the coarse mesh $\mathcal{T}_H$, we can define finite element subspaces similar to the ones defined on the fine mesh, and discretize the original Stokes problem to obtain a linear system of equations

$$A_0 x_0 = b_0.$$

The central-line coarse problem for the 1D model (9) reads as follows: Find $(u_H^{cl}, p_H^{cl}) \in V_H^{cl} \times P_H^{cl}$, such that

$$B_{cl}(u_H^{cl}, p_H^{cl}; v, q) = F_{cl}(v, q) \quad \forall (v, q) \in V_H^{cl} \times P_H^{cl} \tag{11}$$

with

$$B_{cl}(u_H^{cl}, p_H^{cl}; v, q) = \left(K_r u_H^{cl}, v \right) + \left(\frac{A_s}{\rho} \frac{\partial p_H^{cl}}{\partial s}, v \right) - \left(\frac{\partial (A_s u_H^{cl})}{\partial s}, q \right)$$

and

$$F_{cl}(v, q) = (f_{cl}, v).$$

The equivalent matrix form of (11) can be written as

$$A_{cl} x_{cl} = b_{cl}. \tag{12}$$

We next define the restriction and extension operators R_{cl} and E_{cl} between the one-dimensional central-line coarse finite element space $V_H^{cl} \times P_H^{cl}$ and the fine mesh finite element space $V_h \times P_h$ as follows. Let $\{\phi_i^H(x), i = 1, \cdots, m\}$ be the finite element basis functions on the coarse mesh $\mathcal{T}_H$, where m is the total number of coarse

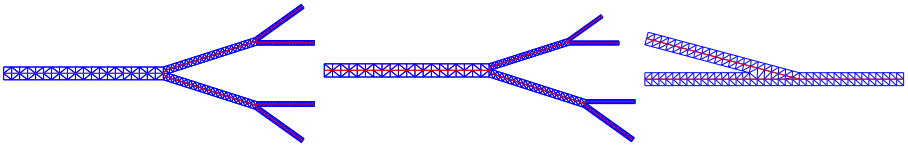

Fig. 6 Three artery-like domains and the coarse mesh (blue) and the central-line coarse mesh (red). Left: symmetric arterial network; middle: asymmetric arterial network; right: confluence artery

mesh points in $\mathcal{T}_H$. Let E_c^f be the coarse finite element space $V_H \times P_H$ to the fine mesh finite element space $V_h \times P_h$ interpolation operator

$$E_c^f = \text{diag}\underbrace{(E, \cdots, E)}_{d+1}, \quad E = [E_1, E_2, \cdots, E_m]^T \tag{13}$$

and

$$E_i = [\phi_i^H(x_1), \phi_i^H(x_2), \cdots, \phi_i^H(x_n)]^T,$$

where $\{x_i\}_{i=1}^n$ is the collection of all mesh points of $\mathcal{T}_h$. The restriction operator R_f^c can be defined as the transpose of E_c^f. Let $\{s_i\}_{i=1}^{m_{cl}}$ and $\{x_j^c\}_{j=1}^m$ be the collections of all mesh points of $\mathcal{T}_H^{cl}$ and $\mathcal{T}_H$, respectively. For each $s_i \in \mathcal{T}_H^{cl}$, denote the cross section of s_i as $C_s(s_i)$. Then, from the definitions of $\mathcal{T}_H^{cl}$ and $\mathcal{T}_H$, it is clear that

$$\text{for any } s_i \in \mathcal{T}_H^{cl}, \text{ there exists a } x_j^c \in \mathcal{T}_H, \text{ such that } x_j^c = x(s_i),$$

and

$$\text{for any } x_j^c \in \mathcal{T}_H, \text{ there exists a } s_i \in \mathcal{T}_H^{cl}, \text{ such that } x_j^c \in C_s(s_i).$$

Using the assumptions (A3) and (A4), we define the restriction from (v_H, p_H) in $V_H \times P_H$ to (v_H^{cl}, p_H^{cl}) in $V_H^{cl} \times P_H^{cl}$ as

$$v_H^{cl}(s_i) = \frac{1}{A_s(s_i)} \int_{C_s(s_i)} v_H(x) \cdot \tau(s_i) d\sigma, \quad p_H^{cl}(s_i) = \frac{1}{A_s(s_i)} \int_{C_s(s_i)} p_H(x) d\sigma \tag{14}$$

for any $s_i \in \mathcal{T}_H^{cl}$ and the extension from (v_H^{cl}, p_H^{cl}) to (v_H, p_H) as

$$v_H(x_j^c) = v_H^{cl}(s_i) \cdot \tau(s_i) V_p\left(\frac{|x_j^c - x(s_i)|}{r_0(s_i)}\right), \quad p_H(x_j^c) = p_H^{cl}(s_i) \tag{15}$$

for any $x_j^c \in \mathcal{T}_H$, where V_p is given in (6) and $s_i \in \mathcal{T}_H^{cl}$ in (15) corresponds to $x_j^c \in C_s(s_i)$. The restriction and extension operators defined in (14)–(15) from the central-line coarse space to the coarse space in R^d are not easily computable, below we introduce R_c^{cl} and E_{cl}^c as a matrix form of the operators that are approximations of (14) and (15), respectively. For simplicity, we only discuss the case $d = 2$. The extension to $d = 3$ is trivial.

Denote by the tangent matrices as $T_k := \text{diag}\left(\tau^k(s_1), \cdots, \tau^k(s_{m_{cl}})\right)$ $(k = 1, 2)$, the restriction weighting coefficients $\{w_{i,j}^r\}_{i=1,j=1}^{m_{cl},m}$ as

$$w_{i,j}^r = \begin{cases} 1/2, & x_j^c = x(s_i) \\ 1/4, & x_j^c \in C_s(s_i), x_j^c \neq x(s_i) \\ 0, & x_j^c \notin C_s(s_i) \end{cases}$$

and the extension weighting coefficients $\left\{w_{i,j}^{e,u}\right\}_{i=1,j=1}^{m_{cl},m}$ and $\left\{w_{i,j}^{e,p}\right\}_{i=1,j=1}^{m_{cl},m}$ for the velocity and pressure, respectively, as

$$w_{i,j}^{e,u} = \begin{cases} 1, & x_j^c = x(s_i) \\ 0, & x_j^c \neq x(s_i) \end{cases}, \quad w_{i,j}^{e,p} = \begin{cases} 1, & x_j^c \in C_s(s_i) \\ 0, & x_j^c \notin C_s(s_i) \end{cases}.$$

Then, we define the restriction matrix R_c^{cl} as

$$R_c^{cl} = \begin{pmatrix} W_1^r & W_2^r & 0 \\ 0 & 0 & W^r \end{pmatrix},\ W_k^r = T_k W^r\ (k = 1, 2),\ W^r = \begin{pmatrix} w_{1,1}^r & \cdots & w_{1,m}^r \\ \vdots & \ddots & \vdots \\ w_{m_{cl},1}^r & \cdots & w_{m_{cl},m}^r \end{pmatrix}$$

and the extension matrix E_c^{cl} as

$$E_{cl}^c = \begin{pmatrix} W_1^{e,u} & W_2^{e,u} & 0 \\ 0 & 0 & W^{e,p} \end{pmatrix}^T,\ W_k^{e,u} = T_k W^{e,u}\ (k = 1, 2)$$

and

$$W^{e,l} = \begin{pmatrix} w_{1,1}^{e,l} & \cdots & w_{1,m}^{e,l} \\ \vdots & \ddots & \vdots \\ w_{m_{cl},1}^{e,l} & \cdots & w_{m_{cl},m}^{e,l} \end{pmatrix}\ (l = u,\ p).$$

Finally, we define $R_{cl} : V_h \times P_h \to V_H^{cl} \times P_H^{cl}$ and $E_{cl} : V_H^{cl} \times P_H^{cl} \to V_h \times P_h$ as

$$R_{cl} = R_c^{cl} R_f^c; \qquad E_{cl} = E_c^f E_{cl}^c. \tag{16}$$

With these multiscale restriction and extension operators, we have the multiscale two-level additive Schwarz preconditioner

$$P_{2s,cl}^{-1} = E_{cl} A_{cl}^{-1} R_{cl} + \sum_{i=1}^{N} R_i^T A_i^{-1} R_i. \tag{17}$$

Remark 4 Instead of the finite element method discussed in the previous section, we can use the parameterized or stabilized finite element method for the 1D model (9) by replacing B_{cl} in (11) with

$$\begin{aligned} B_{cl}^{\beta,\gamma}(u_H^{cl}, p_H^{cl}; v, q) = & \left(K_r u_H^{cl}, v\right) + \left(\frac{A_s}{\rho}\frac{\partial p_H^{cl}}{\partial s}, v\right) - \beta\left(\frac{\partial (A_s u_H^{cl})}{\partial s}, q\right) \\ & -\gamma \sum_{e \in \mathcal{T}_H^{cl}} H_e^2 \left(A_s \frac{\partial p_H^{cl}}{\partial s}, \frac{\partial q}{\partial s}\right)_e, \end{aligned} \tag{18}$$

where $0 < \beta \leq 1$ and $\gamma \geq 0$. Here, the scaling factor β can be used to adjust the convergence rate of the Krylov iteration but does not change the 1D model (9). Because of the stabilization, the pressure part of the residual function on the fine mesh is no longer zero, and therefore, we include a similar stabilization term in the 1D model with an adjustable parameter γ. More details about the choices of β and γ will be discussed in the numerical experiments.

4 Condition number estimates for the elliptic problems in artery-like domain

To estimate the condition number of the proposed method theoretically for the Stokes problem is difficult. In this section, we provide an estimate for the elliptic problems defined on artery-like domains. We consider only the single vessel case. For the arterial network case, we can decompose it into some single vessels and then obtain similar results. In the following, we extend some basic inequalities [39] to the vessel domain case where we assume that the diameter of the vessel is far less than the length of the vessel. In this section, $x \lesssim y$ and $x \approx y$ mean that there exists a positive constants c that is independent of the mesh size, the number of subdomains, and the aspect ratio of the domain such that $x \leq cy$ and $x = cy$, respectively. We consider the elliptic equation in an artery-like domain $\Omega \subset R^d$ $(d = 2, 3)$

$$\begin{cases} -\Delta u = f \ \text{ in } \ \Omega, \\ \quad u = g \ \text{ on } \ \partial\Omega. \end{cases} \tag{19}$$

Let $H_g^1(\Omega) := \left\{v \in H^1(\Omega) : v = g \text{ on } \partial\Omega\right\}$ and $H_0^1(\Omega)$ be the subspace of $H^1(\Omega)$ and vanished on the boundary of Ω. Then, the weak formulation of (19) is written as: Find $u \in H_g^1(\Omega)$ such that

$$a(u, v) = (f, v) \quad \forall v \in H_0^1(\Omega)$$

with $a(u, v) = \int_\Omega \nabla u \nabla v dx$ and $(f, v) = \int_\Omega f v dx$.

Denote by $\|u\|_{0,\Omega}$ as the L^2 norm of the Sobolev space $L^2(\Omega)$ and $|u|_{1,\Omega}$ as the H^1 seminorm of the Sobolev space $H^1(\Omega)$, respectively.

Lemma 1 *Let $\Omega \subset R^d$ $(d = 2, 3)$ be a single vessel with length L and diameter D $(D \lesssim L)$ (see* Fig. 5*). Then, for all $u \in H^1(\Omega)$*

$$\|u\|_{0,\Omega}^2 \lesssim D^2 |u|_{1,\Omega}^2 + D\|u\|_{0,\Gamma}^2, \tag{20}$$

where $\Gamma \subset \partial\Omega$ is the wall of Ω and it has a diameter of order L.

Proof We partition Ω into nonoverlapping subdomains $\{\Omega_i\}_{i=1}^m$ with the diameter $\text{diam}(\Omega_i) \approx D$ and the volume (area) $|\Omega_i| \approx D^d$. Then, for each subdomain Ω_i, using Poincaré-Friedrichs inequality, we have

$$\|u\|_{0,\Omega_i}^2 \lesssim D^2 |u|_{1,\Omega_i}^2 + D\|u\|_{0,\Gamma_i}^2, \tag{21}$$

where $\Gamma_i \subset \partial\Omega_i$ has a diameter of order D. Now summing all subregions $\Omega_i, i = 1, \cdots, m$ and using $\Gamma := \cup_{i=1}^m \Gamma_i$, we complete the proof. □

Lemma 2 *Let Ω be vessel domain with length L and diameter D, and $\{\Omega_i\}_{i=1}^N$ be a nonoverlapping partition of Ω along vessel direction with length L^i and diameter*

$D^i = D$. *Denote by* $\Gamma_{ij} = \bar{\Omega}_i \cap \bar{\Omega}_j$ *as the common edge of* Ω_i *and* Ω_j. *If* $D^i \lesssim L^i$, *then we have*

$$\|u\|^2_{0,\Gamma_{ij}} \lesssim D^i |u|^2_{1,\Omega_i^{\Gamma_{ij}}} + \frac{1}{D^i}\|u\|^2_{0,\Omega_i^{\Gamma_{ij}}}, \tag{22}$$

$$\|u\|^2_{0,\Gamma_{ij}} \lesssim D^j |u|^2_{1,\Omega_j^{\Gamma_{ij}}} + \frac{1}{D^j}\|u\|^2_{0,\Omega_j^{\Gamma_{ij}}}. \tag{23}$$

Here, $\Omega_k^{\Gamma_{ij}} := \left\{x \in \Omega_k : dist(x, \Gamma_{ij}) < diam(\Gamma_{ij})\right\}$ *for* $k = i, j$.

Proof We obtain the results by a direct application of the trace inequality and the scaling argument [39]. □

Lemma 3 *Let* Ω *be vessel domain with length* L *and diameter* D. *Let* $\left\{\Omega_i^\delta\right\}_{i=1}^N$ *be an overlapping decomposition of* Ω *with overlapping size* δ. Ω_i^δ *is obtained by extending* Ω_i *with the size* δ *along the vessel direction. Denote* $\Omega_{ij}^\delta = \bar{\Omega}_i^\delta \cap \bar{\Omega}_j^\delta$. *We assume that* $D^i \approx D^j$, $L^i \approx L^j$ *and* $\delta \lesssim D^i$. *If* $D^i \lesssim L^i$, *then we have*

$$\begin{aligned}\|u\|^2_{0,\Omega_{ij}^\delta} \lesssim\ & \delta^2\left(1 + \frac{D^i}{\delta}\right)\left(|u|^2_{1,\Omega_i^{\Gamma_{ij}}} + |u|^2_{1,\Omega_j^{\Gamma_{ij}}}\right) \\ & + \frac{\delta}{D^i}\left(\|u\|^2_{0,\Omega_i^{\Gamma_{ij}}} + \|u\|^2_{0,\Omega_j^{\Gamma_{ij}}}\right),\end{aligned} \tag{24}$$

where $\Omega_k^{\Gamma_{ij}}, k = i, j$ *is defined as in Lemma 2.*

Proof Let $\Omega_k^o = \Omega_{ij}^\delta \setminus \Omega_k, k = i, j$ and then we have that $\Omega_{ij}^\delta = \Omega_i^o \cup \Omega_j^o$. Using Lemma 1, we first have

$$\|u\|^2_{0,\Omega_{ij}^\delta} = \|u\|^2_{0,\Omega_i^o} + \|u\|^2_{0,\Omega_j^o} \lesssim \delta^2|u|^2_{1,\Omega_i^o} + \delta\|u\|^2_{0,\Gamma_{ij}} + \delta^2|u|^2_{1,\Omega_j^o} + \delta\|u\|^2_{0,\Gamma_{ij}}.$$

Then, using $\delta \lesssim D^i$ and Lemma 2, we obtain the desired estimate (24). □

In the following, let $V_h \subset H_0^1(\Omega)$ and $V_h^i \subset H_0^1(\Omega_i^\delta)$ be the piecewise linear continuous finite element spaces with mesh size h, I^h the standard interpolation operator associated with V_h, and $a_i(u, v) = \int_{\Omega_i^\delta} \nabla u \nabla v dx$ for all $u, v \in H_0^1(\Omega_i^\delta)$ and $i \in \{1, \cdots, N\}$. Then, we have the stable decomposition result for the vessel domain.

Lemma 4 *Let* Ω, Ω_i, *and* Ω_i^δ *be the same as in the previous lemma. Let* $\{\theta_i\}_{i=1}^N$ *be the partition of unit that satisfies* $\sum_{i=1}^N \theta_i = 1, 0 \le \theta_i \le 1$ *and* $|\nabla\theta_i| \le \frac{1}{\delta}$. *For* $u \in V_h$, *we set* $u_i = I^h(\theta_i(u)) \in V_h^i$. *If* $D^i \lesssim L^i$ *and* $D^i \approx D$, *then we have* $u = \sum_{i=1}^N u_i$ *and*

$$\sum_{i=1}^N a_i(u_i, u_i) \lesssim \left(1 + \frac{D}{\delta}\right) a(u, u). \tag{25}$$

Proof The decomposition of u can be derived directly:

$$u = I^h \sum_{i=1}^{N} \theta_i(u) = \sum_{i=1}^{N} u_i. \tag{26}$$

For the stability of the decomposition, using the properties of θ_i and Poincaré inequality, we have

$$\begin{aligned} a_i(u_i, u_i) &= |I^h(\theta_i u)|^2_{1,\Omega_i^\delta} \lesssim |\theta_i u|^2_{1,\Omega_i^\delta} \lesssim \int_{\Omega_i^\delta} |u\nabla\theta_i|^2 + \int_{\Omega_i^\delta} |\theta_i \nabla u|^2 \\ &\lesssim \int_{\Omega_{ij}^\delta} |u\nabla\theta_i|^2 + \int_{\Omega_i^\delta} |\nabla u|^2 \lesssim \frac{1}{\delta^2} \int_{\Omega_{ij}^\delta} |u|^2 + |u|^2_{1,\Omega_i^\delta} \\ &\lesssim \left(1 + \frac{D^i}{\delta}\right)\left(|u|^2_{1,\Omega_i^\delta} + |u|^2_{1,\Omega_j^\delta}\right) + \frac{1}{\delta D^i}\left(||u||0,\, \Omega_i^{\Gamma_{ij}\,2} + ||u||0,\, \Omega_j^{\Gamma_{ij}\,2}\right) \\ &\lesssim \left(1 + \frac{D^i}{\delta}\right)\left(|u|^2_{1,\Omega_i^\delta} + |u|^2_{1,\Omega_j^\delta}\right) + \frac{D^i}{\delta}\left(|u|1,\, \Omega_i^{\delta\,2} + |u|1,\, \Omega_j^{\delta\,2}\right) \\ &\lesssim \left(1 + \frac{D^i}{\delta}\right)\left(|u|^2_{1,\Omega_i^\delta} + |u|^2_{1,\Omega_i^\delta}\right). \end{aligned} \tag{27}$$

Finally, summing over all subdomains, we have

$$\begin{aligned} \sum_{i=1}^{N} a_i(u_i, u_i) &\lesssim \max_i \left(1 + \frac{D^i}{\delta}\right) \sum_{i=1}^{N} |u|^2_{1,\Omega_i^\delta} \\ &\lesssim \left(1 + \frac{D}{\delta}\right) a(u, u). \end{aligned} \tag{28}$$

□

Remark 5 Consider the situation that Ω is an arterial network consisting of m connected single vessels $\{\Omega_i\}_i^m$. For each vessel Ω_i, we denote the length and the diameter as L_i and D_i. If we partition each vessel Ω_i into N_i overlapping subdomains $\{\Omega_{ij}^\delta\}_{j=1}^{N_i}$ as in the previous discussion, then from Lemma 4, we obtain a similar result

$$\sum_{i=1}^{m} \sum_{j=1}^{N_i} a_{ij}(u_{ij}, u_{ij}) \lesssim \max_i \left(1 + \frac{D_i}{\delta}\right) a(u, u)$$

as in the single vessel case.

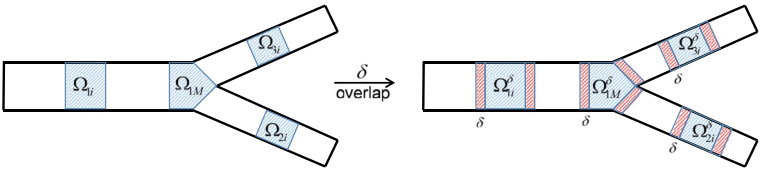

Fig. 7 Some simple nonoverlapping subdomains (left) and overlapping subdomains (right), and the overlapping extensions are along the vessel direction(s)

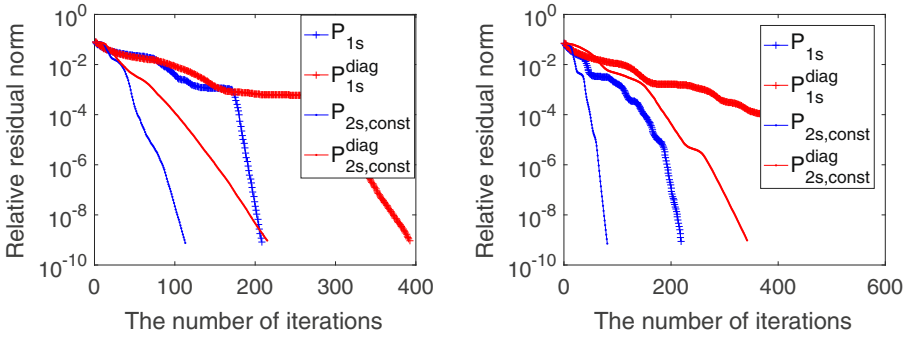

Fig. 8 The number of iterations of fully coupled (blue) and decoupled (red) Schwarz preconditioners for Stokes problem in the single vessel (left) and the symmetric arterial network (right). Here P_{1s} and P_{1s}^{diag} correspond to the fully coupled and block-diagonal one-level Schwarz preconditioners, and $P_{2s,const}$ and $P_{2s,const}^{diag}$ correspond to the fully coupled and block-diagonal two-level Schwarz preconditioners with piecewise constant coarse space, respectively

By Lemma 4, Remark 5, and the abstract Schwarz theory [39], we obtain the following estimate of the condition number.

Theorem 1 *Let A be the matrix form of $a(u, v)$ and P_{1s}^{-1} be the one-level additive Schwarz preconditioner of A. If Ω is an artery-like domain, each subdomain has a diameter that is less than or approximately equal to its length, then the condition number of $P_{1s}^{-1}A$ satisfies*

$$\kappa(P_{1s}^{-1}A) \leq O\left(1 + \frac{D}{\delta}\right),$$

where $D = \max_{1 \leq i \leq m} D_i$ and the hidden constant does not depend on the mesh size, the number of subdomains and the aspect ratio of the domain.

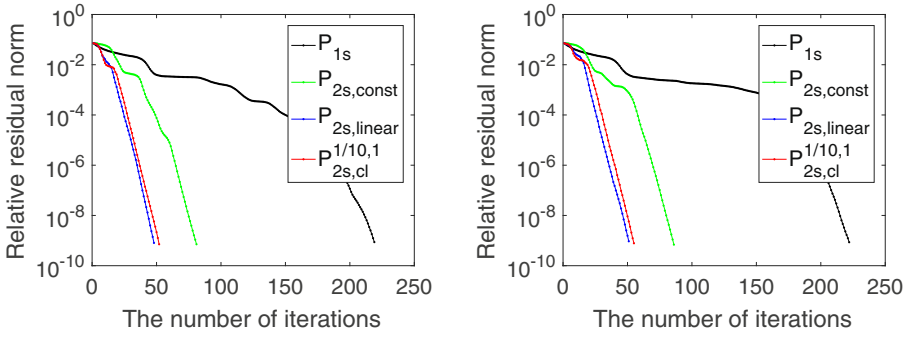

Fig. 9 The number of iterations of the different preconditioners for the arterial network cases. Left: symmetric arterial network; right: asymmetric arterial network

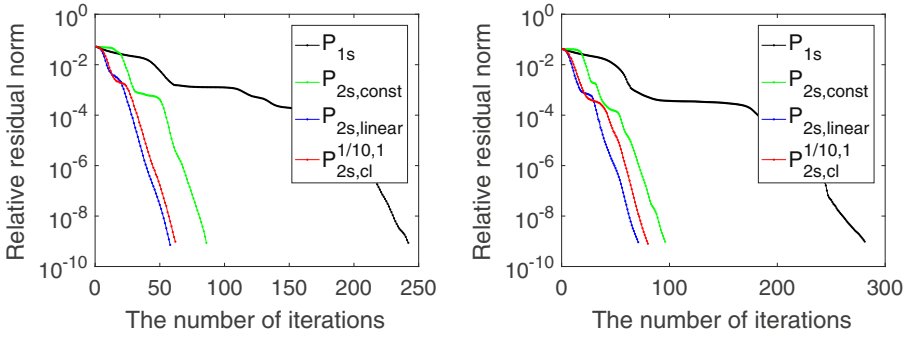

Fig. 10 The number of iterations of the different preconditioners with finer mesh sizes for the symmetric arterial network case. Left: $h = 0.05$, $\delta = 2h$; right: $h = 0.025$, $\delta = 4h$

Remark 6 For problems with the Dirichlet boundary condition, the coarse space is not always necessary because the Poincaré inequality holds without requiring the mean value of the function defined on all subdomains.

5 Numerical experiments

In this section, we present some numerical experiments to show the efficiency and robustness of the central-line coarse preconditioner for Stokes problems in arteries. In addition, we also study the scalability of the one-level additive Schwarz preconditioner for elliptic problem. We consider several configurations including a single vessel domain $\Omega = (0, 25) \times (-0.5, 0.5)$ and arteries with different bifurcations such as symmetric, asymmetric arterial networks and confluence artery (see Fig. 6). We divide the artery Ω into $N = mM$ nonoverlapping subdomains $\{\Omega_{ij}\}_{i=1,j=1}^{m,M}$, where m is the number of vessels without bifurcation $\{\Omega_i\}_{i=1}^{m}$ and M is the number of nonoverlapping subdomains $\{\Omega_{ij}\}_{j=1}^{M}$ of each vessel Ω_i. Denote by $\{\Omega_{ij}^{\delta}\}_{i=1,j=1}^{m,M}$ as the overlapping partition of Ω (see Fig. 7). In the following experiments, denote by h the fine mesh size and set the overlapping size $\delta = h$, and we also set $M = 100$ for the single vessel and $M = 20$ for the arterial networks and also the confluence artery.

Table 1 The number of iterations of the central-line coarse preconditioner with different parameter γ for the single vessel case

β	1/5						1/10					
γ	1	1/5	1/10	1/50	1/100	0	1	1/5	1/10	1/50	1/100	0
Iter	119	98	94	90	89	91	116	93	88	83	82	87

Table 2 The number of iterations of the central-line coarse preconditioner with different parameter β for the single vessel case

γ	1						0					
β	1	1/2	1/5	1/10	1/20	1/50	1	1/2	1/5	1/10	1/20	1/50
Iter	136	127	119	116	113	110	114	103	91	87	96	120

5.1 The Stokes problem

In this subsection, we consider the Stokes problem (1). We assume the source function $f = 0$ and the boundary conditions are given as follows. For the velocity, we assume the fluid is no-slip on the wall and satisfies some parabolic profiles on the inlet and outlet(s). Note that the parabolic profile is determined uniquely by the value at the center of the inlet or outlets, and the values are selected carefully to guarantee the conservation of flux. For the pressure variable, we prescribe its value at the center point of the inlet. We discretize the Stokes problem (1) with a stabilized $P_1 - P_1$ finite element method with $h = 0.1$ and then solve the resulting algebraic systems using a right preconditioned GMRES method. The stopping condition for GMRES is that the relative residual norm is less than 10^{-9} and the subdomain problems are solved exactly.

For comparison, we also report some experiments with the regular coarse preconditioner $P_0^{-1} = E_c^f A_0^{-1} R_f^c$ introduced in Section 3.2, and the piecewise constant coarse preconditioner $P_{const}^{-1} = E_{const} A_{const}^{-1} R_{const}$, where $A_{const} = R_{const} A E_{const}$ and R_{const} satisfies

$$R_{const} = \text{diag}\,\underbrace{(Z, \cdots, Z)}_{d+1}, \quad Z = \left[1_{\Omega_{11}}, \cdots, 1_{\Omega_{1M}}, \cdots, 1_{\Omega_{m1}}, \cdots, 1_{\Omega_{mM}}\right]^T.$$

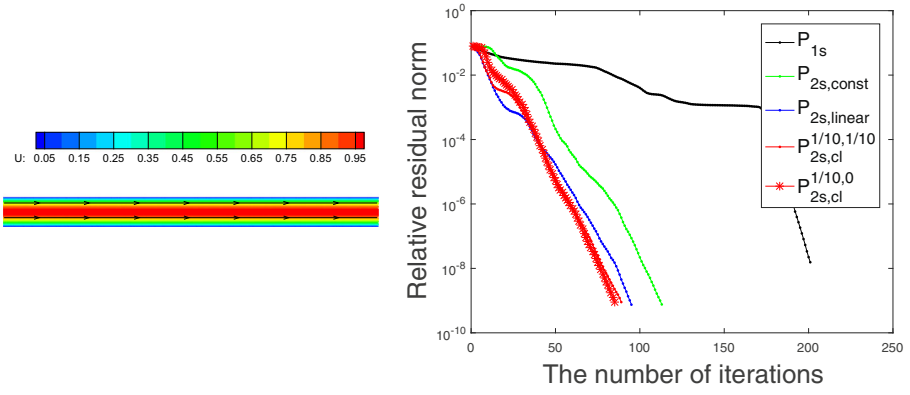

Fig. 11 The streamline and the number of iterations of different preconditioners with and without the stabilization term for the single vessel case

Table 3 The number of iterations of the cental-line coarse preconditioner with different γ for the symmetric arterial network case

γ	4	2	1	1/5	1/10	1/20	1/100	1/1000	0
Iter	81	78	76	77	78	80	82	83	102

Here, $1_{\Omega_{ij}}$ is a column vector whose values are ones for the fine mesh points in Ω_{ij} and zeros for others for all i and j and E_{const} is the transpose of R_{const}. Then denote by $P^{-1}_{2s,const} = P^{-1}_{const} + P^{-1}_{1s}$ and $P^{-1}_{2s,linear} = P^{-1}_{0} + P^{-1}_{1s}$ as the corresponding two-level preconditioners.

First, we compare the number of iterations of the fully coupled and the block-diagonal (fully decoupled) additive Schwarz preconditioners in the single vessel and the symmetric arterial network cases in Fig. 8. It is clear that the fully coupled one- and two-level preconditioners are more effective than the block-diagonal preconditioners [21]. Therefore, we only consider the fully coupled preconditioner in the rest of the paper.

For the next set of experiments, we denote by $P^{-1\,\beta,\gamma}_{2s,cl}$ as the central-line coarse preconditioner with parameters β and γ in $B^{\beta,\gamma}_{cl}$ (18). In Fig. 9, we show the residual history of four methods including the one-level method, two two-level methods, and the central-line method. In terms of the number of iterations, the two-level method with the regular coarse space is the fastest which is also the most expensive method in terms of the amount of arithmetics operations. The second best is the central-line preconditioner which is the cheapest, and surprisingly, its number of iterations is just a little larger than the regular coarse space. The piecewise constant coarse method is not too far behind, and the one-level method is not competitive with the other three. Fig. 10 shows the number of iterations for finer mesh sizes and the results are similar, as long as the overlap is proportional to the diameter of the subdomain.

To further understand the effect of the parameters β and γ for the central-line coarse preconditioner, we summarize the results for the single vessel case in Tables 1 and 2. When β is fixed, we can see from Table 1 that a small γ or even zero (means no stabilization term) produces the smallest number of iterations. Table 2 shows the number of iterations with different β with fixed γ. Figure 11 provides a comparison of the central-line coarse preconditioner with suitable parameters β and γ and the other two coarse preconditioners for the single vessel case. For the arterial network case, Table 3 shows that the impact of γ is not as big as β, $\gamma = 1$ is a good choice for this case, as shown in Table 4 with different choices of β.

Table 4 The number of iterations of the central-line coarse preconditioner with different β for the symmetric arterial network

β	1	1/2	1/4	1/6	1/8	1/10	1/20	1/100
Iter	76	62	53	51	50	51	59	78

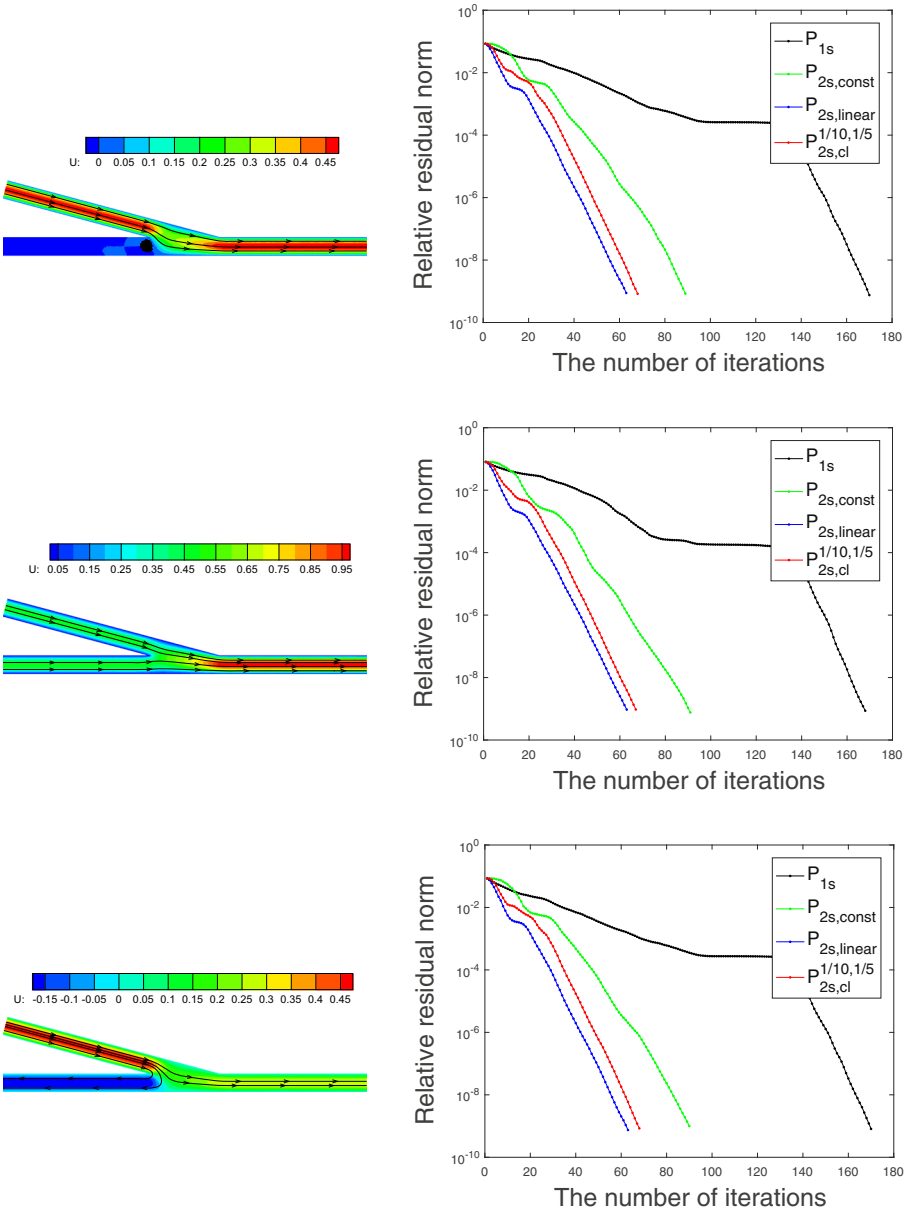

Fig. 12 Three streamlines (left) and the corresponding number of iterations of different preconditioners for the confluence artery case (right). Top: the clogged flow, middle: the confluence flow; bottom: the divergence flow

Next, we consider the confluence artery (see the right figure of Fig. 6). Even though the geometry involves a bifurcation, but we do not apply condition (10). Instead, we simply discretize the 1D model (9) in entire confluence artery (see the

right figure of Fig. 4). The geometry has three openings, and by assigning different inlet/outlet, we can simulate a few different flow situations. In the left figures of Fig. 12, we assign the top-left and right boundaries as the inlet and outlet, respectively, and then consider three situations for the lower-left boundary: (1) the clogged flow which assumes that the lower-left boundary is a non-flow boundary; (2) the confluence flow which assumes that the lower-left boundary is an inlet; (3) the divergence flow which assumes that the lower-left boundary is an outlet. In the right figures of Fig. 12, we show the corresponding number of iterations of the central-line coarse preconditioner and the other three preconditioners. The fluids are more complex than the single vessel case, but the performance of the central-line preconditioner is quite well for all these situations.

Furthermore, we consider the bifurcation condition (10). We compare two discretizations of the 1D model; one without using (10), and one using (10) with $\xi_2 = 1/2, \xi_3 = 1/2$. We use subscripts "global" and "local" to represent these two discretizations. The results are summarized in Fig. 13, and it shows that these two discretizations offer roughly the same number of iterations; thus, we conclude that (10) is not necessary. It shows that these two discretized ways result in nearly the same number of iterations, which means that such an inexact solve for the 1D coarse model in the bifurcation of the artery does not affect the efficiency of the central-line coarse preconditioner.

Finally, we compare the dimension of different coarse spaces for the arterial networks with different number of junctions in Table 5. The dimension of the central-line coarse space is much smaller than the dimension of the other two coarse spaces, especially the regular coarse space, which means that the central-line coarse preconditioner requires less memory and CPU time in each iteration compared with the other preconditioners, especially for the high-dimensional and realistic arterial networks with many branches. We can also see in Table 5 and Fig. 14 that the number of iterations of the central-line coarse preconditioner is a little larger than that of the regular coarse preconditioner, but not for the piecewise constant coarse preconditioner.

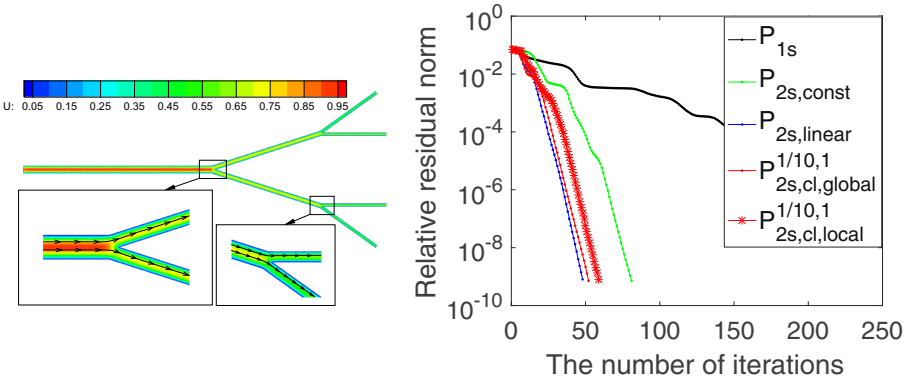

Fig. 13 The contour of x-axis component of velocity and the number of iterations of different preconditioners for the symmetric arterial network case

Table 5 The comparison of the dimension of different coarse spaces and its number of iterations (in parentheses) for the arterial networks with different number of branches

Junctions	$P_{2s,const}$	$P_{2s,linear}$	$P_{2s,cl}$
2^0-1	300	909	202
	(112)	(94)	(84)
2^2-1	420	1296	294
	(80)	(47)	(51)
2^4-1	1860	5730	1302
	(201)	(68)	(82)

5.2 The elliptic problem

In this subsection, we present some numerical experiments for the elliptic problem (19) in artery-like domain Ω. We consider the following boundary condition and right-hand side

$$g = sin(x)y + 10 \text{ on } \partial\Omega; \quad f = -\Delta(sin(x)y + 10) = sin(x)y \text{ in } \Omega.$$

For the symmetry and asymmetry arterial networks, the diameter D_i and the length L_i of each vessel Ω_i satisfy $\frac{D_i}{L_i} = \frac{1}{25}$. We consider the one-level additive Schwarz preconditioner P_{1s}^{-1} and two two-level additive Schwarz preconditioners $P_{2s,const}^{-1}$ and $P_{2s,linear}^{-1}$. In Table 6, we show results for different values of M and N, and in all the cases, we have $\frac{2}{25} \leq \frac{D_{ij}}{L_{ij}} \leq \frac{30}{25}$. The experiments show that the number of iterations of the one-level Schwarz preconditioner does not change much for $D_{ij} \lesssim L_{ij}$ and it outperforms both two-level methods. For elliptic problems on arterial-like domains, the coarse space preconditioner is not necessary, which is consistent

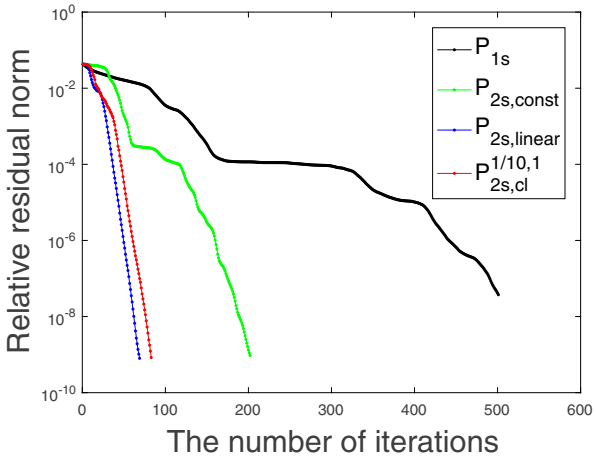

Fig. 14 The number of iterations of the different preconditioners for the symmetric arterial network with 2^4-1 junctions and $h = 0.03$, $\delta = 4h$

Table 6 The number of iterations of the one- and two-level additive Schwarz preconditioners for the elliptic problem with Dirichlet boundary condition in arterial networks

Artery type	symmetry arterial network					asymmetry arterial network				
M	2	5	10	20	30	2	5	10	20	30
N	14	35	70	140	210	14	35	70	140	210
P_{1s}	10	10	10	11	13	10	11	11	11	13
$P_{2s,const}$	12	14	14	14	15	12	14	14	14	15
$P_{2s,linear}$	12	12	13	13	13	12	13	13	13	13

with the theoretical result in Theorem 1, but this is not true for Stokes problems that require a coarse preconditioner for the algorithm to be scalable.

6 Some final remarks

When simulating blood flows in arterial networks on parallel computers, a coarse preconditioner is often necessary to couple the subproblems solved on different processors in order to have the desired parallel scalability. When the geometry of the artery becomes complex, a suitable coarse space is sometimes difficult to design and the corresponding system is expensive to solve. In this paper, we take the advantage of the fact the artery looks one-dimensional, and introduce a simple, but surprisingly powerful, central-line coarse preconditioner that can be integrated into the regular one-level additive Schwarz preconditioner via suitable multiscale interpolation and restriction operators constructed by preserving the boundary geometry of the fine mesh. The computational cost of the one-dimensional preconditioner is very low compared with existing methods, and the number of iterations is almost the same as the high dimensional coarse preconditioners. Only two-dimensional Stokes problems are considered in this paper. The extensions to three-dimensional Stokes and Navier-Stokes equations in realistic arteries will be our next step.

References

1. Bai, Z.Z., Golub, G.H.: Accelerated Hermitian and skew-Hermitian splitting iteration methods for saddle-point problems. IMA J. Numer. Anal. **27**(1), 1–23 (2007)
2. Benzi, M., Gander, M.J., Golub, G.H.: Optimization of the Hermitian and skew-Hermitian splitting iteration for saddle-point problems. BIT Numer. Math. **43**(5), 881–900 (2003)
3. Benzi, M., Golub, G.H.: A preconditioner for generalized saddle point problems. SIAM J. Matrix Anal. Appl. **26**(1), 20–41 (2004)
4. Benzi, M., Golub, G.H., Liesen, J.: Numerical solution of saddle point problems. Acta Numer. **14**, 1–137 (2005)
5. Bramble, J.H., Pasciak, J.E., Vassilev, A.T.: Analysis of the inexact Uzawa algorithm for saddle point problems. SIAM J. Numer. Anal. **34**(3), 1072–1092 (1997)
6. Čanić, S.: Blood flow through compliant vessels after endovascular repair: wall deformations induced by the discontinuous wall properties. Comput. Vis. Sci. **4**(3), 147–155 (2002)

7. Douglas, J., Wang, J.P.: An absolutely stabilized finite element method for the Stokes problem. Math. Comput. **52**(186), 495–508 (1989)
8. Elman, H.C.: Multigrid and Krylov subspace methods for the discrete Stokes equations. Int. J. Numer. Methods Fluids **22**(8), 755–770 (1996)
9. Elman, H.C., Golub, G.H.: Inexact and preconditioned Uzawa algorithms for saddle point problems. SIAM J. Numer. Anal. **31**(6), 1645–1661 (1994)
10. Formaggia, L., Gerbeau, J.F., Nobile, F., Quarteroni, A.: On the coupling of 3D and 1D Navier–Stokes equations for flow problems in compliant vessels. Comput. Methods Appl. Mech. Eng. **191**(6-7), 561–582 (2001)
11. Formaggia, L., Lamponi, D., Quarteroni, A.: One-dimensional models for blood flow in arteries. J. Eng. Math. **47**(3-4), 251–276 (2003)
12. Formaggia, L., Nobile, F., Quarteroni, A.: A One Dimensional Model for Blood Flow: Application to Vascular Prosthesis. In: Mathematical Modeling and Numerical Simulation in Continuum Mechanics, pp. 137–153. Springer (2002)
13. Formaggia, L., Nobile, F., Quarteroni, A., Veneziani, A.: Multiscale modelling of the circulatory system: a preliminary analysis. Comput. Vis. Sci. **2**(2-3), 75–83 (1999)
14. Gander, M., Xu, Y.: Optimized Schwarz methods with nonoverlapping circular domain decomposition. Mathematics of Computation **86** (2017)
15. Gander, M.J., Xu, Y.: Optimized Schwarz methods for circular domain decompositions with overlap. SIAM J. Numer. Anal. **52**(4), 1981–2004 (2014)
16. Gigante, G., Pozzoli, M., Vergara, C.: Optimized Schwarz methods for the diffusion-reaction problem with cylindrical interfaces. SIAM J. Numer. Anal. **51**(6), 3402–3430 (2013)
17. Gunzburger, M.D.: Finite element methods for viscous incompressible flows: a guide to theory, practice, and algorithms. Elsevier (2012)
18. Hughes, T.J., Franca, L.P.: A new finite element formulation for computational fluid dynamics: VII. The Stokes problem with various well-posed boundary conditions: symmetric formulations that converge for all velocity/pressure spaces. Comput. Methods Appl. Mech. Eng. **65**(1), 85–96 (1987)
19. Hughes, T.J., Franca, L.P., Balestra, M.: A new finite element formulation for computational fluid dynamics: V. Circumventing the babuška-brezzi condition: a stable Petrov-Galerkin formulation of the Stokes problem accommodating equal-order interpolations. Comput. Methods Appl. Mech. Eng. **59**(1), 85–99 (1986)
20. Kim, H.H., Lee, C.O., Park, E.H.: A FETI-DP formulation for the Stokes problem without primal pressure components. SIAM J. Numer. Anal. **47**(6), 4142–4162 (2010)
21. Klawonn, A.: An optimal preconditioner for a class of saddle point problems with a penalty term. SIAM J. Sci. Comput. **19**(2), 540–552 (1998)
22. Klawonn, A.: Block-triangular preconditioners for saddle point problems with a penalty term. SIAM J. Sci. Comput. **19**(1), 172–184 (1998)
23. Klawonn, A., Pavarino, L.F.: Overlapping Schwarz methods for mixed linear elasticity and Stokes problems. Comput. Methods Appl. Mech. Eng. **165**(1-4), 233–245 (1998)
24. Klawonn, A., Pavarino, L.F.: A comparison of overlapping Schwarz methods and block preconditioners for saddle point problems. Numer. Linear Algebra Appl. **7**(1), 1–25 (2000)
25. Kong, F., Cai, X.C.: A highly scalable multilevel Schwarz method with boundary geometry preserving coarse spaces for 3D elasticity problems on domains with complex geometry. SIAM J. Sci. Comput. **38**(2), C73–C95 (2016)
26. Kong, F., Cai, X.C.: A scalable nonlinear fluid–structure interaction solver based on a Schwarz preconditioner with isogeometric unstructured coarse spaces in 3D. J. Comput. Phys. **340**, 498–518 (2017)
27. Lee, J., Smith, N.: Development and application of a one-dimensional blood flow model for microvascular networks. Proc. Inst. Mech. Eng. Part H: J. Eng. Med. **222**(4), 487–511 (2008)
28. Li, J.: A dual-primal FETI method for incompressible Stokes equations. Numer. Math. **102**(2), 257–275 (2005)
29. Li, J., Widlund, O.: BDDC Algorithms for incompressible Stokes equations. SIAM J. Numer. Anal. **44**(6), 2432–2455 (2006)
30. Pavarino, L.F.: Indefinite overlapping Schwarz methods for time-dependent Stokes problems. Comput. Methods Appl. Mech. Eng. **187**(1-2), 35–51 (2000)
31. Pavarino, L.F., Widlund, O.: Balancing Neumann-Neumann methods for incompressible Stokes equations. Commun. Pure Appl. Math. J. Issued Cour. Inst. Math. Sci. **55**(3), 302–335 (2002)

32. Quarteroni, A., Formaggia, L.: Mathematical modelling and numerical simulation of the cardiovascular system. Handb. Numer. Anal. **12**, 3–127 (2004)
33. Quarteroni, A., Manzoni, A., Vergara, C.: The cardiovascular system: mathematical modelling, numerical algorithms and clinical applications. Acta Numer. **26**, 365–590 (2017)
34. Shapiro, A.H.: Steady flow in collapsible tubes. J. Biomech. Eng. **99**(3), 126–147 (1977)
35. Sherwin, S., Formaggia, L., Peiro, J., Franke, V.: Computational modelling of 1D blood flow with variable mechanical properties and its application to the simulation of wave propagation in the human arterial system. Int. J. Numer. Methods Fluids **43**(6-7), 673–700 (2003)
36. Sherwin, S., Franke, V., Peiro, J., Parker, K.: One-dimensional modelling of a vascular network in space-time variables. J. Eng. Math. **47**(3-4), 217–250 (2003)
37. Smith, N., Pullan, A., Hunter, P.: An anatomically based model of transient coronary blood flow in the heart. SIAM J. Appl. Math. **62**(3), 990–1018 (2002)
38. Streeter, V.L., Keitzer, W.F., Bohr, D.F.: Pulsatile pressure and flow through distensible vessels. Circ. Res. **13**(1), 3–20 (1963)
39. Toselli, A., Widlund, O.: Domain decomposition methods algorithms and theory. Springer, Berlin (2005)
40. Verfürth, R.: A multilevel algorithm for mixed problems. SIAM J. Numer. Anal. **21**(2), 264–271 (1984)
41. Wittum, G.: Multi-grid methods for Stokes and Navier-Stokes equations. Numer. Math. **54**(5), 543–563 (1989)